Science Bulletin xxx (xxxx) xxx

Contents lists available at ScienceDirect

Science Bulletin

journal homepage: www.elsevier.com/locate/scib

Article

Coupled sleep rhythm disruption predicts cognitive decline in Alzheimer's disease

Tao Wei [a,1], Jianyang Zhou [b,d,1], Zhibin Wang [a,1,*], Xiaoduo Liu [a], Yingxin Mi [a], Yiwei Zhao [a], Yi Xing [a], Bo Zhao [a], Shaojiong Zhou [a], Yufei Liu [a], Yunzhe Liu [c,d,*], Yi Tang [a,e,*]

[a] Department of Neurology & Innovation Center for Neurological Disorders, Xuanwu Hospital, Capital Medical University, National Center for Neurological Disorders, Beijing 100053, China
[b] School of Basic Medical Sciences, Capital Medical University, Beijing 100069, China
[c] State Key Laboratory of Cognitive Neuroscience and Learning, IDG/McGovern Institute for Brain Research, Beijing Normal University, Beijing 100875, China
[d] Chinese Institute for Brain Research, Beijing 102206, China
[e] Key Laboratory of Neurodegenerative Diseases, Ministry of Education of the People's Republic of China, Beijing 100053, China

ARTICLE INFO

Article history:
Received 28 December 2024
Received in revised form 7 February 2025
Accepted 11 February 2025
Available online xxxx

Keywords:
Alzheimer's disease
Sleep
Slow oscillation
Spindle
Theta burst
Cognitive decline
Biomarker

ABSTRACT

The effect of sleep on memory consolidation depends on the precise interaction of slow oscillations (SOs), theta bursts, and spindles. Disruption in coupling of these sleep rhythms has been reported for individuals with Alzheimer's disease (AD). However, it is unknown how the sleep rhythms evolve during AD progression and whether disrupted sleep rhythms facilitate cognitive decline in AD. Here, we analyze data of 93 individuals from sleep electroencephalography (EEG), MRI, cerebrospinal fluid (CSF) AD biomarkers, and two-year cognitive assessments among three populations: AD dementia (n = 33), mild cognitive impairment (MCI) due to AD (n = 38), and cognitively normal (CN, n = 22). Our study identifies the evolving pattern of coupled sleep rhythm disruption with advancing cognitive stages in AD. Specifically, the frequency of SO-theta burst coupling and SO-spindle coupling decreases from CN to MCI; SO-theta burst coupling and SO-spindle coupling further misalign from MCI to AD dementia. The *APOE* ε4 allele and elevated amyloid and tau burden are associated with coupled sleep rhythm disruption. Hippocampal and medial prefrontal cortex atrophy are respectively linked to disruption of SO-theta burst coupling and SO-spindle coupling. Notably, coupled sleep rhythm disruption predicts accelerated cognitive decline over a two-year follow-up period. Our study presents that integrating sleep EEG with CSF and MRI biomarkers enhances the predictive ability for AD progression, which unravels the potential of sleep rhythms as monitoring and interventional targets for AD.

1. Introduction

Sleep is essential in reinstating memory and maintaining brain health [1–3]. During non-rapid eye movement (NREM) sleep, coupled sleep rhythms—comprising slow oscillations (SOs; < 1.25 Hz), theta bursts (4–8 Hz), and spindles (12–16 Hz)—precede hippocampal sharp wave ripples in service of memory formation [1,4,5]. Physiologically, coupled sleep rhythms prompt the transfer of memory traces through hippocampal-cortical networks by cross-regional communications. Alzheimer's disease (AD) is a neurodegenerative disorder characterized by progressive cognitive decline, affecting memory, executive functions, language, and visuospatial skills. In addition to cognitive impairment, alterations in sleep architecture, including disrupted coupled sleep rhythms, have been observed in AD [6]. Changes in slow wave sleep percentage were measured across repeated overnight sleep studies conducted, on average, 5.2 years apart (range: 4.8–7.1 years). After the second PSG assessment, participants were followed for up to 17 years to assess the risk of incident all-cause dementia and exhibited a 27 % increased risk of cognitive decline during this time [7]. However, it remains unclear how coupled sleep rhythms evolve across different stages of AD or whether their disruption actively contributes to cognitive decline in AD individuals.

Current theories in neuroscience propose that coupled sleep rhythms during NREM sleep support memory consolidation [8].

* Corresponding authors.
E-mail addresses: wangzhibinxw@163.com (Z. Wang), yunzhe.liu@bnu.edu.cn (Y. Liu), tangyi@xwhosp.org (Y. Tang).
[1] Those authors contributed equally to this work.

https://doi.org/10.1016/j.scib.2025.03.023

An influential model proposes that sequential coupling of SO and spindles sets a timeframe for hippocampal sharp wave ripples to occur during NREM sleep [1,9,10]. In particular, the depolarizing 'up-states' of the SO coupled to spindles are proposed to facilitate ripple expression, which subsequently nests into spindle troughs [2,5]. Theta burst activity has been found to drive SOs and to precede hippocampal sharp wave ripples [11,12]. The temporal precision of coupled sleep rhythms orchestrates neural processing and communication during NREM sleep [13]. The neuroanatomical basis for SO and theta burst coupling is thought to emerge from hippocampo-cortical communication [11,14], while SO and spindle coupling is thought to reflect thalamo-cortical communication [5,15]. Communication between these brain regions during NREM sleep is known to participate in memory processing [16–18]. In AD pathology, amyloid plaques and neurofibrillary tangles are preferentially aggregated at brain regions that function in memory processing during sleep [19]. The misalignment of coupled sleep rhythms is associated with early amyloid-β accumulation in the prefrontal cortex and predicts memory decline in healthy older adults [20]. Although longitudinal data on coupled sleep rhythms and cognition in AD remain limited, emerging evidence suggests that disrupted sleep rhythms during NREM sleep may contribute to cognitive decline during AD progression. We hypothesized that the frequency and misalignment of specific NREM sleep rhythms (i.e., SO-theta burst coupling, SO-spindle coupling) are closely related to the rate of cognitive decline across different stages of AD.

In this study, we examined the properties of two aspects of coupled sleep rhythms (i.e., SO and theta burst coupling, SO and spindle coupling) among three populations: AD dementia, mild cognitive impairment (MCI) due to AD, and cognitively normal (CN) populations. We hypothesized that coupled sleep rhythms during NREM sleep are progressively disrupted with advancing cognitive stages, which would correlate with AD neurobiological features (i.e., *APOE* genotype, MRI, core AD biomarkers) and cognitive functions. To determine the impact of coupled sleep rhythm disruption on cognitive function, we assessed two-year longitudinal changes in cognitive function among the three populations. Our results identify a clear relationship between coupled sleep rhythm disruption and longitudinal decline in cognitive function with advancing cognitive stages in AD, which unravels the potential of sleep rhythms as monitoring and interventional targets for AD.

2. Methods

Memory reactivation relies on the precise temporal coordination of NREM sleep oscillations [1,4,5]. Evidence from individuals with AD indicates that these coupled sleep rhythms are disrupted, with reduced theta burst power during the SO phase and an earlier peak in spindle power during the rising phase of the SO, suggesting a link to AD pathology [21]. However, AD involves complex mechanisms that extend beyond sleep physiology, encompassing genetic predispositions, amyloid and tau pathology, and structural brain alterations. Consequently, a longitudinal approach is necessary to capture how disruptions in coupled sleep rhythms evolve alongside established genetic, cerebrospinal fluid (CSF), and MRI markers, and to clarify whether these factors collectively predict cognitive decline over time. Guided by these considerations, we integrated electrophysiological, genetic, CSF, and MRI assessments into our study design, aiming to comprehensively evaluate changes in coupled sleep rhythms and cognition in the context of AD progression.

2.1. Enrolled individuals

Ninety-three individuals (mean [standard deviation] age: 66.6 [8.4] years; 62 females) participated in the study. Seventeen additional participants were excluded because of not enough sleep or sleep disorders (Fig. S1 online). The sample size needed for power = 0.8 and type I error rate = 5% was calculated based on prior human memory research study [22] (Table S1 online). All participants underwent comprehensive clinical and cognitive assessments, including baseline neuropsychological testing and the Clinical Dementia Rating (CDR) scale. A subset of 74 participants completed a two-year follow-up CDR assessment. Participants were grouped by amyloid positivity and CDR status: 22 were CN based on global CDR score of 0 and amyloid-negative by [^{18}F] AV45 amyloid-β-PET; 38 were diagnosed with MCI based on a global CDR score of 0.5 and amyloid-positive imaging; and 33 had AD dementia with CDR scores between 1 and 2 and amyloid-positive imaging. CN participants were also screened for subjective cognitive decline, while MCI participants presented either subjective or objective cognitive impairments with relatively preserved daily living activities [23]. AD participants met NIA-AA criteria for probable AD [24], as confirmed by a dementia specialist. Exclusion criteria included other significant neurological conditions, sleep disorders (e.g., insomnia, obstructive sleep apnea, periodic limb movement disorder), psychiatric disorders (e.g., substance dependence, major depression), or medications known to affect cognition or sleep. All participants reported good quality sleep. Ethical approval was received from Xuanwu Hospital, Capital Medical University (No. 2024251) in accordance with the Declaration of Helsinki. The informed consent from all participants was obtained.

2.2. Experimental protocol

At baseline, participants underwent subcutaneous blood draws, CSF collection via lumbar puncture, and amyloid PET imaging. A comprehensive neuropsychological evaluation was conducted by trained professionals. Eligible participants were given an 8-hour sleeping chance according to their habitual sleep schedule, monitored via polysomnography under controlled conditions. Structural MRI scans were performed on part of the participants. Two years later, a follow-up CDR assessment was conducted by the same neuropsychological team.

2.3. Neuropsychological assessment

Cognitive function was evaluated using a battery of tests, including the CDR Scale, WHO-UCLA Auditory Verbal Learning Test (AVLT) for memory; the Digit Span Test (DST) and Trail Making Test (TMT) for attention and executive function; the Clock Drawing Test (CDT) for visuospatial skills; the Boston Naming Test (BNT) for language; and the Mini-Mental State Examination (MMSE) and Montreal Cognitive Assessment (MoCA) for global cognition. Cognitive decline in this study is operationally defined by increases in the CDR-sum of boxes (CDR-SB). The CDR-SB assesses six core domains—memory, orientation, judgment and problem-solving, social functioning, home and hobbies, and self-care—into a single score, providing a comprehensive measure of cognitive and functional impairment (https://knightadrc.wustl.edu/professionals-clinicians/cdr-dementia-staging-instrument/). Notably, the CDR-SB is frequently used to track early-stage progression of AD and captures a broader range of cognitive and daily functioning changes beyond memory alone.

2.4. CSF biomarker acquisition and analysis

CSF samples were collected following international guidelines. Lumbar punctures were performed at 8:00 a.m. using a 22-gauge Sprotte needle. After low-speed centrifugation, samples were aliquoted into polypropylene tubes. CSF was analyzed on the same day for amyloid-β42, amyloid-β40, total tau (t-tau), and

phosphorylated tau 181 (p-tau 181) using enzyme-linked immunosorbent assay (ELISA) kits from Fujirebio (Ghent, Belgium).

2.5. Serum collection and APOE genotyping

Venous blood samples were drawn in the morning after a 12-hour fast and centrifuged at 2000 × *g* for 10 min to obtain serum stored at −80 °C until analysis. Genome DNA was extracted from blood accordingly to the salting-out method with modifications. *APOE* genotyping was performed via restriction enzyme digestion, as previously described. Participants were classified as *APOE* ε4 carriers if they had at least one ε4 allele (e.g., ε3/ε4 or ε4/ε4).

2.6. MRI acquisition

MRI data was acquired on a 3.0 T Siemens scanner. Two high-resolution T1-weighted anatomical images were obtained using a 3D MPRAGE protocol with the following parameters: repetition time, 2300 ms; echo time, 2.4 ms; flip angle, 8°; field of view, 256 mm; matrix size, 256 × 256; slice thickness, 1.0 mm; 176 slices. MPRAGE images were co-registered, and the mean image was used for optimized voxel-based morphometry (VBM) to assess grey matter volume in specific regions of interest (ROI).

2.7. Structural MRI data analysis

To assess grey matter volume, optimized VBM was performed using SPM8 (Wellcome Department of Imaging Neuroscience) with the VBM8 toolbox (http://dbm.neuro.unijena.de/vbm.html) and the Diffeomorphic Anatomical Registration through Exponentiated Lie algebra (DARTEL) toolbox to enhance registration accuracy for older brains to the normalized MNI template [25,26]. Two T1-weighted MPRAGE images were co-registered and averaged to improve the signal-to-noise ratio. These averaged images were then segmented using a Markov random field approach [27], followed by registration, normalization, and modulation using DARTEL. Grey and white matter segmentations were input into DARTEL to create a study-specific template, which was used for normalizing individual brains to MNI space. The resulting modulated grey matter maps were smoothed with an 8 mm Gaussian kernel. Total intracranial volume (TIV) was calculated for each participant by summing grey matter, white matter, and CSF volumes, and TIV-adjusted grey matter volumes were used in subsequent analyses to control for head size differences. Given the importance of the prefrontal cortex, thalamus, and hippocampus in sleep oscillations, spindles, and theta bursts, regions of interest (ROIs) were generated for these areas using the Anatomical Automatic Labeling repository [28] within the Wake Forest University PickAtlas toolbox [29]. Grey matter volumes within these ROIs, as well as an occipital control region, were extracted using the Marsbar toolbox and analyzed in relation to sleep and memory metrics.

2.8. Sleep monitoring and EEG data acquisition

Overnight PSG monitoring was conducted for each participant between 9:00 p.m. and 6:00 a.m. in the neurology department, following standard protocols established by the AASM. PSG recordings included continuous EEG monitoring from nineteen leads based on the international 10–20 system (Fp1, Fp2, F3, F4, F7, F8, FZ, C3, C4, CZ, T3, T4, P3, P4, PZ, T5, T6, O1, and O2), all referenced to the mastoids. Additional physiological signals were recorded to ensure comprehensive sleep assessment, including nasal and oral airflow via thermistors, thoracic and abdominal excursion using strain gauges, and oxygen saturation through finger pulse oximetry. Electrooculography (EOG), electromyography (EMG), and electrocardiography (ECG) were also recorded to monitor eye movements, muscle activity, and heart rate, respectively. Data were recorded using the Grael system (Compumedics, Australia) with a sampling rate of 256 Hz.

2.9. EEG analysis

Analysis was performed using FieldTrip [30], EEGLAB [31], and MNE-python [32]. Preprocessing: EEG and EOG signals were processed using a band-pass filter with a range of 0.1–40 Hz, while EMG signals underwent band-pass filtering between 10–100 Hz followed by a band-stop filter at 50 Hz. Prior to analysis, all signals were down-sampled to 100Hz. Visual inspection and an automated artifact rejection algorithm using the median absolute deviation (MAD) identified and excluded artifacts. Sleep stages were classified offline based on central channel data, following American Academy of Sleep Medicine guidelines. A trained expert annotated sleep stages. SO detection: SOs were automatically detected using EEG data from the C3 electrode during NREM sleep. NREM data were band-pass filtered between 0.16 and 1.25 Hz using a third-order two-pass FIR filter. Events meeting both a duration criterion (0.8–2 s) and an amplitude criterion (the top 25% of events by amplitude) were identified. Artifact-free epochs (± 2 s around the SO trough) were extracted for analysis. Theta burst and spindle identification: Theta bursts and spindles were detected automatically using EEG data from the C3 electrode filtered between 4–8 Hz for theta bursts and 12–16 Hz for spindles with a third-order two-pass FIR filter [5,21] (Fig. S2 online). An amplitude threshold (75th percentile of the root mean square value) and window length (0.5–3.0 s) were applied to define events. Artifact-free epochs (± 2 s around the theta burst/spindle peak) were extracted for analysis. Time-frequency analysis: Time-frequency representations (TFRs) for each event epoch were computed using the mtmconvol function from the FieldTrip toolbox, covering 1–30 Hz with 1 Hz steps and three cycles using a 10 ms sliding Hanning window. TFRs were normalized across the entire time range and averaged for each participant and population. Baseline-normalized EEG power was quantified within predefined TF windows. Theta bursts were analyzed between 4–8 Hz at −0.5 to 0.2 s from the SO trough, and spindle power was measured between 12–16 Hz at 0.3–1.3 s from the SO trough [21] (Fig. S3 online). Preferred phase-amplitude coupling (PAC) phases: PAC refers to the phenomenon wherein the amplitude of a high-frequency oscillation (e.g., in the theta or spindle range) is modulated by the phase of a lower-frequency oscillation (e.g., SO), indicating cross-frequency interaction. The preferred SO phase refers to the phase angle of the slow oscillation where the power of the burst or spindle reaches its maximum. To determine the precise phase of the SO at which theta burst, or spindle peak amplitudes occurred, we extracted SO phase values for each participant at all recorded time points within SO-theta burst or SO-spindle coupling events using the Hilbert transform. This allowed us to identify the exact SO phase at the moment of peak theta burst or spindle activity. For each participant, the phase values corresponding to theta burst or spindle peak amplitudes were calculated and then averaged to produce a mean phase value. To statistically compare mean phase values across participant populations, we applied the Watson-Williams multi-sample test, a robust method for analyzing circular data. This test allowed us to evaluate whether the mean SO phase values associated with theta burst or spindle peaks significantly differed between populations. Peri-event time histograms (PETHs): PETHs illustrate the average neural activity (e.g., EEG power or spike rate) within a specified time window around a particular event, enabling

temporal alignment of physiological signals with behavioral or neural events [5]. To clarify the temporal relationships between event types, PETHs were generated. These histograms visualized the timing of a "target" event relative to a "seed" event, such as showing the occurrence of SO troughs in relation to spindle peaks, with the spindle peak marked as the seed event at time zero. For each participant, histograms were created using MATLAB's 'hist' function with 100-ms bins spanning from −5 to +5 seconds relative to the seed event. These histograms were then averaged across participants in each population to illustrate a representative temporal pattern of event relationships (Fig. S4 online). To investigate how theta burst and spindle power vary with SO phase, we first binned each trial's data into 18 SO-phase bins. This procedure produced a single SO-binned theta burst histogram and a single SO-binned spindle histogram per trial. We then normalized each phase-power distribution by dividing the mean power in each bin by the total power across all bins.

2.10. Statistical analysis

Demographic and clinical data were compared across the three populations using analysis of variance (ANOVA) for continuous variables and χ^2 tests for categorical data. If global testing was significant, post hoc comparisons were performed using Bonferroni correction for continuous data and pairwise χ^2 tests with Benjamini-Hochberg correction for categorical variables. EEG variables were compared using ANCOVA, adjusting for age, gender, education, and *APOE* ε4 carrier status. Mann-Whitney *U* tests were employed to evaluate differences in baseline and follow-up CDR scores.

Non-uniformity of preferred SO phases for theta bursts and spindles was assessed with the Rayleigh test (CircStat toolbox), while Cohen's d was used to report effect sizes for Watson-Williams tests (circular ANOVA equivalent). Paired *t*-tests were conducted to examine whether the mean power of theta bursts and spindles in specific SO phase bins was significantly higher than in other bins, based on visual inspection of the SO-binned power distribution histogram. Circular-linear correlations (CircStat toolbox) were applied to investigate the nonlinear relationship between preferred phases and clinical variables (e.g., MRI and neuropsychological scores). Linear regressions, adjusted for age, gender, education, and *APOE* ε4 carrier status, were used to explore associations between EEG variables (frequency and power) and clinical measures.

We performed an integrated multivariate analysis using Canonical Correlation Analysis (CCA) to examine the relationship between EEG variables during NREM sleep and neuropsychological scores. To mitigate the risk of overfitting, we initially applied Principal Component Analysis (PCA) to reduce the dimensionality of both EEG variables and neuropsychological scores, selecting the number of components that accounted for 80% of the variance. CCA was then applied to identify statistically significant pairs of canonical variables, calculate their correlation coefficients, and assess the contribution of the original variables to these canonical components. A permutation test (n = 10,000) was subsequently conducted to assess the reliability of the CCA results by randomly shuffling participant labels and re-running CCA to generate a valid null distribution. Finally, we computed the correlation between the canonical variables and all original variables to better understand the relationships between EEG variables during NREM sleep and neuropsychological scores.

To further assess the impact of coupled sleep rhythm on cognitive outcomes in AD, linear regression models (adjusted for age, sex, education, and *APOE* ε4 carrier status) were employed to explore associations between coupled sleep rhythm and CDR-SB and CDR-memory scores. Logistic regression models were used to investigate relationships between coupled sleep rhythms and CDR-global score exacerbation, with the same adjustments. The area under the ROC curve (AUC), sensitivity, and specificity were calculated to assess the predictive capacity of EEG biomarkers for CDR-global score worsening.

The significance level of $P < 0.05$ (two-tailed) was applied for all tests. Data analysis was performed using SPSS (version 27, IBM Corp.) and MATLAB (2018b).

3. Results

3.1. Participant characteristics

A total of 93 individuals were included in this study (AD dementia = 33, MCI = 38, CN = 22). Demographic and clinical characteristics were detailed in Table 1. There were no significant differences among the populations in terms of age, sex distribution, or education level. The *APOE* ε4 allele was more prevalent in the AD dementia and MCI populations compared to the CN population (AD dementia: 48.5%; MCI: 42.1%; CN:22.7%). The AD dementia and MCI populations showed lower CSF Aβ42/Aβ40 ratios and higher CSF p-tau181 and t-tau levels compared to the CN population (all *P*corrected <0.01). Neuropsychological scores were lower in the AD dementia and MCI populations, with the exception of Forward Digit Span (Table 1). Sleep staging metrics were consistent across the three populations (Table S2 online). Regarding overall NREM sleep, the AD dementia and MCI populations each showed significant reductions in the frequency (number per minute) of SOs, theta bursts, and spindles compared to the CN population (Table 1).

3.2. Coupled sleep rhythm during NREM sleep is disrupted in AD dementia and MCI

To assess how coupled sleep rhythms are disrupted during AD progression, we first used ANCOVA models to compare the frequency of SO-theta burst coupling and SO-spindle coupling among the AD dementia, MCI, and CN populations (adjusted for age, gender, education, and *APOE* ε4 carrier status). The AD dementia and MCI populations had significantly decreased frequency of SOs, theta bursts, and spindles in SO-theta burst and SO-spindle couplings compared to the CN population (all $P_{\text{corrected}} < 0.05$, Table 1; Fig. 1a, d and Fig. S5 online). Notably, such differences in the frequency of sleep rhythms were not found in uncoupled SOs, theta bursts and spindles (Fig. 1d). These findings suggest that: i) coupled sleep rhythm disruption is a pathophysiological feature in the context of AD progression; ii) the frequency of coupled sleep rhythms decreases in the AD dementia and MCI populations.

We next investigated changes in the power of sleep rhythms in SO-theta burst and SO-spindle couplings during AD progression by calculating the normalized power of theta bursts and spindles among the three populations (Fig. 1b, c). ANCOVA models indicated that SO-coupled theta burst and spindle power significantly decreased in the MCI population (adjusted for age, gender, education, and *APOE* ε4 carrier status; theta burst: MD = −0.07, $P_{corrected}$ = 0.023; spindle: MD = −0.07, $P_{\text{corrected}}$ = 0.016; Fig. 1e) compared to the CN population. In the AD dementia population, SO-coupled theta burst power further declined compared to the MCI population (MD = −0.06, $P_{\text{corrected}}$ = 0.034; Fig. 1e).

We then explored changes in the temporal precision of coupled sleep rhythms during AD progression, specifically by computing the preferred SO phases coupled to the peak power of theta bursts and spindles among the three populations. Watson-Williams tests showed significant differences between the AD dementia and MCI populations in the preferred SO phases for coupled theta bursts (AD dementia: 87.7° ± 58.6°, MCI: 118.7° ± 40.9°; $F_{1,69}$ = 5.67,

Table 1
Demographic and sleep characteristics.

	CN (n = 22)	MCI (n = 38)	AD dementia (n = 33)	P	Post hoc
Demographics					
Age at sleep study (years), Mean (SD)	64.7 (5.8)	66.4 (11.3)	67.9 (5.2)	0.380	–
Females, n (%)	16 (72.3)	25 (65.6)	21 (63.6)	0.774	–
Education (years), Mean (SD)	11.5 (3.1)	12.5 (3.5)	11.0 (3.0)	0.113	–
Number of *APOE* ε4-positive (%)	5 (22.7)	16 (42.1)	16 (48.5)	0.045	–
CSF AD biomarkers					
Aβ42/Aβ40 ratio, Mean (SD)	0.09 (0.01)	0.07 (0.02)	0.05 (0.02)	<0.001	C > M > A
P-tau181 (pg/ml), median (IQR)	53.8 (34.7–63.7)	80.8 (43.7–141.6)	78.2 (49.9–110.4)	0.005	M A > C
Total tau (pg/ml), median (IQR)	180.3 (140.1–271.4)	404.7 (174.8–789.6)	446.2 (321.8–643.5)	<0.001	M A > C
Neuropsychological test					
CDR-SB, median (IQR)	0.0 (0.0–0.0)	2.3 (0.5–3.0)	5.0 (3.8–8.3)	<0.001	A > M > C
MMSE, Mean (SD)	28.6 (1.0)	24.8 (3.7)	17.6 (4.5)	<0.001	C > M > A
MoCA, Mean (SD)	26.3 (1.9)	20.5 (4.7)	13.1 (4.4)	<0.001	C > M > A
AVLT-Immediate recall, median (IQR)	24.0 (19.0–29.5)	20.5 (16.0–24.0)	12.0 (8.0–16.0)	<0.001	C M > A
AVLT-Delay recall, median (IQR)	10.0 (7.0–11.0)	4.0 (1.0–8.0)	0.0 (0.0–3.0)	<0.001	C > M > A
AVLT-Clue recall, median (IQR)	10.5 (8.8–12.3)	8.0 (4.0–9.3)	3.0 (1.0–5.0)	<0.001	C > M > A
AVLT-Recognition recall, median (IQR)	12.0 (10.8–13.0)	10.0 (7.0–12.0)	6.0 (1.0–9.5)	<0.001	C M > A
CDT, median (IQR)	3.0 (3.0–3.0)	2.0 (2.0–3.0)	1.0 (1.0–2.0)	<0.001	C > M > A
FDS, Mean (SD)	8.3 (1.1)	7.6 (1.4)	7.3 (1.5)	0.053	–
BDS, Mean (SD)	5.1 (1.2)	4.4 (1.3)	3.3 (0.8)	<0.001	C M > A
TMT-A (s), median (IQR)	56.0 (40.0–68.5)	61.5 (46.0–82.8)	103.0 (73.0–150.0)	<0.001	C M > A
TMT-B (s), median (IQR)	69.0 (55.8–84.3)	92.5 (79.5–166.5)	240.0 (150.0–300.0)	<0.001	C > M > A
BNT, Mean (SD)	25.1 (2.6)	22.4 (5.0)	18.6 (4.6)	<0.001	C M > A
Sleep event features					
SO					
Frequency (1 min), Mean (SD)	6.7 (0.9)	5.8 (1.7)	6.4 (0.9)	0.016	C > M
Amplitude (μV), median (IQR)	59.1 (47.7–67.0)	52.3 (43.1–69.2)	44.1 (40.2–57.1)	0.040	C > A
Theta burst					
Frequency (1 min), Mean (SD)	7.1 (0.5)	6.9 (0.6)	6.5 (0.6)	0.011	C M > A
Amplitude (μV), median (IQR)	16.7 (14.1–18.8)	17.0 (13.9–18.5)	15.7 (12.6–19.3)	0.927	–
Spindle					
Frequency (1 min), Mean (SD)	9.1 (1.3)	8.5 (1.2)	8.1 (1.6)	0.045	C > A
Amplitude (μV) -median (IQR)	10.0 (8.6 –12.0)	9.6 (7.5–11.0)	8.2 (7.0–10.4)	0.547	–
SO-theta burst coupling					
Frequency (1 min), Mean (SD)	2.1 (0.5)	1.7 (0.6)	1.6 (0.4)	0.005	C > M A
SO Amplitude (μV), median (IQR)	62.8 (50.7–73.1)	58.7 (46.6–79.0)	50.2 (43.8–61.8)	0.051	–
Theta burst Amplitude (μV), median (IQR)	17.8 (14.9–20.2)	17.9 (14.7–19.7)	17.3 (13.3–20.4)	0.874	–
SO-spindle coupling					
Frequency (1 min), Mean (SD)	1.8 (0.4)	1.5 (0.5)	1.4 (0.4)	0.003	C > M A
SO Amplitude (μV), median (IQR)	58.8 (49.7–70.0)	56.9 (44.3–70.4)	49.3 (42.6–60.5)	0.077	–
Spindle Amplitude (μV), median (IQR)	10.1 (8.8–11.9)	9.8 (8.0–11.2)	8.3 (7.3–10.7)	0.667	–
Uncoupled event frequency					
Theta burst (1 min), Mean (SD)	4.9 (0.4)	5.2 (0.7)	4.9 (0.4)	0.170	–
Spindle (1 min), Mean (SD)	7.4 (1.1)	7.0 (1.1)	6.6 (1.3)	0.390	–

Continuous data are presented as mean (SD) or median (IQR), and categorical variables as numbers (percentage). C > M > A: CN estimates greater than MCI, and MCI estimates greater than AD dementia; M A > C: MCI and AD dementia estimates greater than CN; C M > A: CN and MCI estimate greater than AD dementia; C > A: CN estimates greater than AD dementia; A > M > C: AD dementia estimates greater than MCI, and MCI estimates greater than CN; C > M: CN estimates greater than MCI; C > M A: CN estimates greater than MCI and AD dementia. Statistical significance was assessed using ANCOVA for sleep characteristics, adjusting for age, sex, education, *APOE* ε4 carrier status, and multiple comparisons. AD: Alzheimer's disease; *APOE:* apolipoprotein E; AVLT: Auditory Verbal Learning Test; BDS: Backward Digit Span; BNT: Boston Naming Test; CDR-SB: Clinical Dementia Rating sum of boxes; CDT: Clock Drawing Test; CN: cognitively normal; CSF: cerebrospinal fluid; FDS: Forward Digit Span; IQR: interquartile range; MCI: mild cognitive impairment; MMSE: Mini-Mental State Examination; MoCA: Montreal Cognitive Assessment; SD: standard deviation; SO: slow oscillation; TMT: Trail Making Test.

$P_{corrected}$ = 0.034) and spindles (AD dementia: −43.5° ± 38.2°, MCI: −17.6° ± 37.8°; $F_{1,69}$ = 7.76, $P_{corrected}$ = 0.007) (Fig. 1f, g). Such differences in SO phases were found between the MCI and CN populations. To characterize the distribution of theta burst and spindle power along the SO phase, we binned theta burst and spindle power by SO phase (18 bins) and averaged SO-binned theta burst/spindle distributions for each population (Fig. 1h, i). The AD dementia population showed a distinct pattern in both theta burst and spindle power distribution compared to the CN population (paired-samples t-tests: theta burst: AD dementia, t_{32} = −4.23, $P_{corrected}$ < 0.001; MCI, t_{37} = −0.10, $P_{corrected}$ = 0.902; CN, t_{21} = −3.38, $P_{corrected}$ = 0.003; spindle: AD dementia, t_{32} = −3.67, $P_{corrected}$ < 0.001; MCI, t_{37} = −0.53, $P_{corrected}$ = 0.600; CN, t_{21} = −3.71, $P_{corrected}$ = 0.001). These results suggest that coupled sleep rhythms are misaligned in the AD dementia population. The trends for both N2 and N3 sleep were consistent with our primary analysis of total NREM sleep (Fig. S6 and Table S3 online).

Collectively, our results identify an evolving pattern of coupled sleep rhythms during AD progression: i) the frequency of SO-theta burst coupling and SO-spindle coupling decreases from CN to MCI; ii) SO-theta burst coupling and SO-spindle coupling further misalign from MCI to AD dementia.

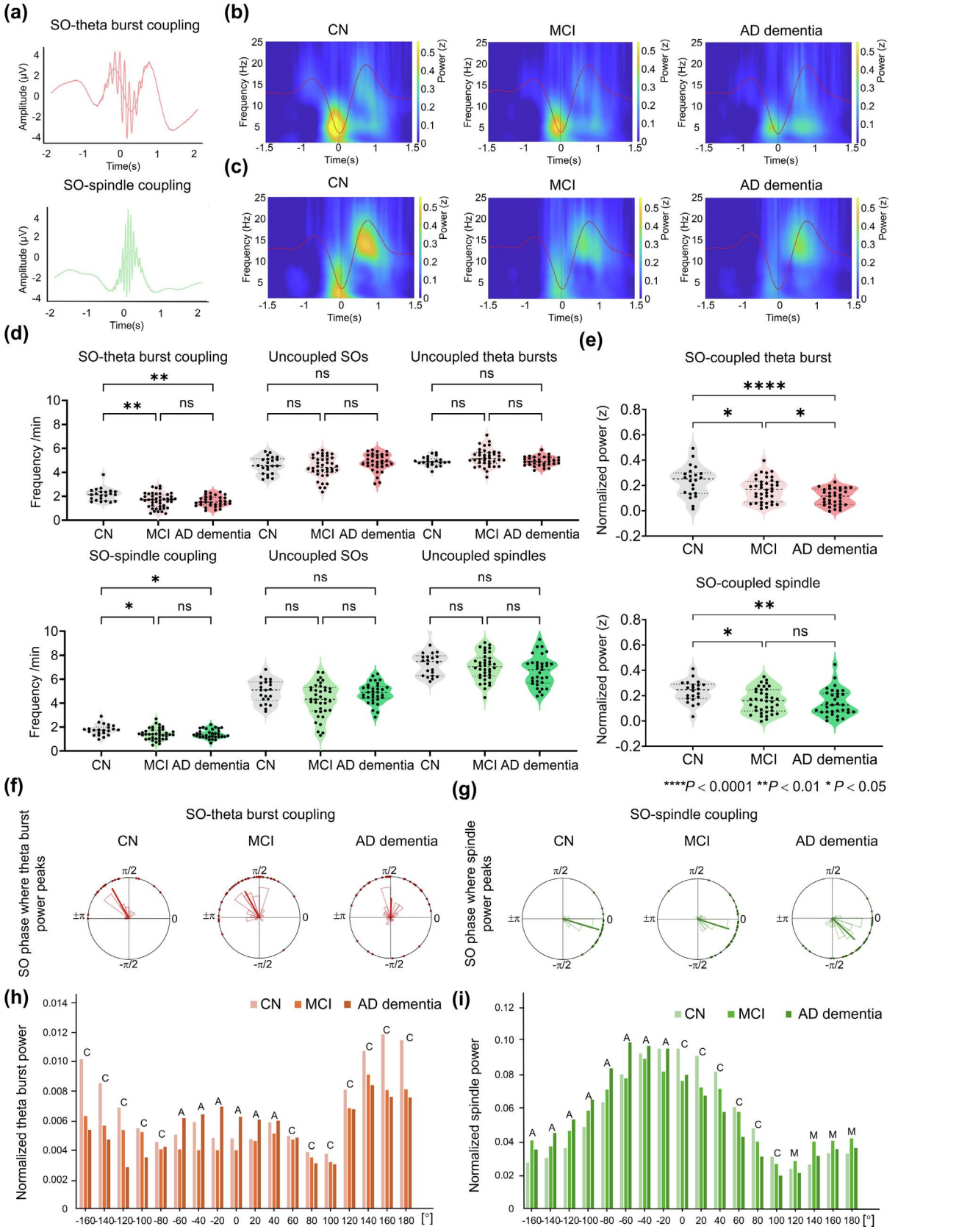

Fig. 1. Coupled sleep rhythms during NERM sleep in the AD dementia, MCI, and CN populations. (a) Conceptual illustration of theta burst (red) and spindle (green) events individually coupled with SO. (b) Averaged time-frequency plots of SO-theta burst coupling for the AD dementia, MCI, and CN populations, with SO superimposed. (c) Same as (b), but for SO-spindle coupling. (d) Violin plots depicting the frequency of SO-theta burst coupling and SO-spindle coupling for the three populations. (e) Violin plots showing SO-coupled theta burst and spindle power for the three populations. (f) Polar histogram of SO phase at the theta burst power peak for the three populations. (g) Same as (f), but for SO phase at the spindle power peak. (h) Histogram of SO-binned theta burst power distributions for the three populations. (i) Same as (h), but for spindle power. Statistical significance for panels (d) and (e) was assessed using ANCOVA, adjusting for age, sex, education, *APOE* ε4 carrier status, and multiple comparisons. AD: Alzheimer's disease; *APOE*: apolipoprotein E; CN: cognitively normal; MCI: mild cognitive impairment; NREM: non-rapid eye movement sleep; SO: slow oscillation.

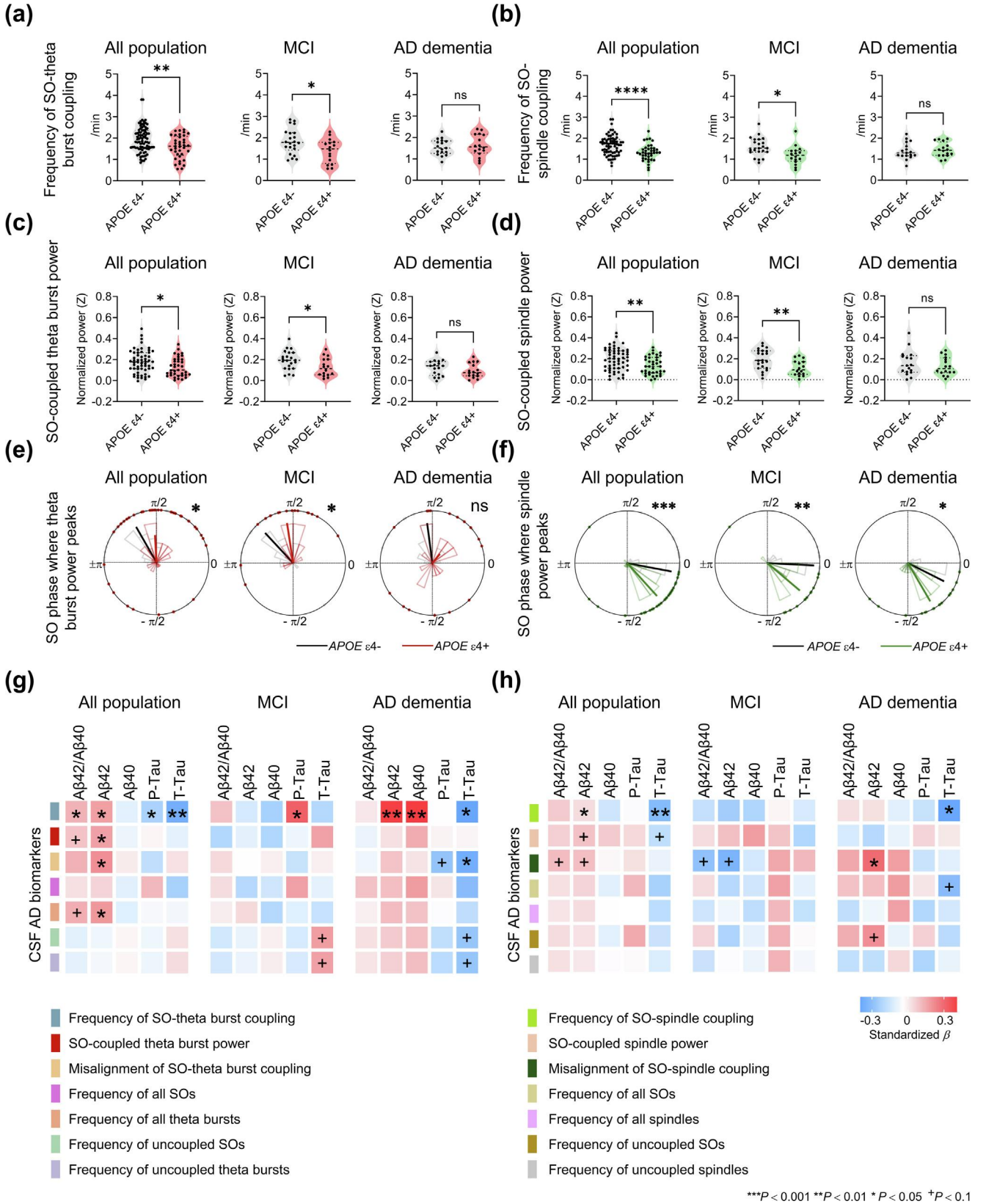

Fig. 2. Associations of coupled sleep rhythm with *APOE* genotype and AD pathology. (a) Violin plots showing the frequency of SO-theta burst coupling between *APOE* ε4 carriers and non-carriers. (b) Same as (a), but for SO-spindle coupling. (c) Violin plots depicting SO-coupled theta burst power in *APOE* ε4 carriers vs. non-carriers. (d) Same as (c), but for SO-coupled spindle power. (e) Polar histogram of preferred SO phases for the coupled theta burst power peak in *APOE* ε4 carriers vs. non-carriers. (f) Same as (e), but for the spindle power peak. (g) Heatmap of associations between SO-theta burst coupling and CSF biomarker levels. (h) Same as (g), but for SO-spindle coupling. Statistical significance was assessed using ANCOVA for panels (a–d), Watson-Williams test for panels (e–f), and linear regression for panels (g–h), adjusting for age, sex, education, *APOE* ε4 carrier status, and multiple comparisons. AD: Alzheimer's disease; *APOE*: apolipoprotein E; CSF: cerebrospinal fluid; MCI: mild cognitive impairment; NREM: non-rapid eye movement Sleep; SO: slow oscillation.

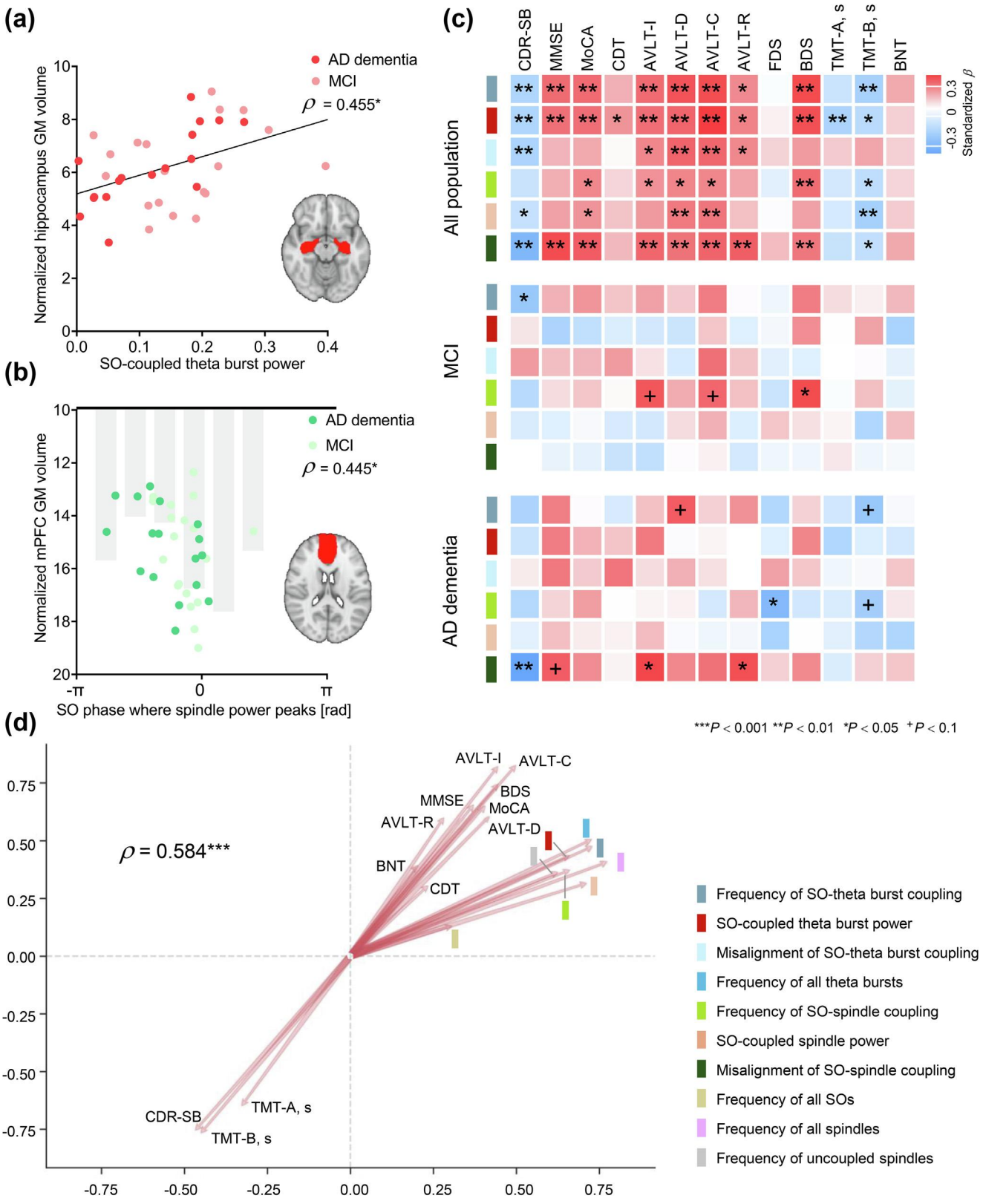
(a)
AD dementia
MCI
ρ = 0.455*
Normalized hippocampus GM volume
SO-coupled theta burst power
(b)
AD dementia
MCI
ρ = 0.445*
Normalized mPFC GM volume
SO phase where spindle power peaks [rad]
(c)
CDR-SB
MMSE
MoCA
CDT
AVLT-I
AVLT-D
AVLT-C
AVLT-R
FDS
BDS
TMT-A, s
TMT-B, s
BNT
All population
MCI
AD dementia
Standardized β
***P < 0.001 **P < 0.01 *P < 0.05 +P < 0.1
(d)
ρ = 0.584***
AVLT-I
AVLT-C
MMSE
BDS
MoCA
AVLT-R
AVLT-D
BNT
CDT
CDR-SB
TMT-A, s
TMT-B, s
Frequency of SO-theta burst coupling
SO-coupled theta burst power
Misalignment of SO-theta burst coupling
Frequency of all theta bursts
Frequency of SO-spindle coupling
SO-coupled spindle power
Misalignment of SO-spindle coupling
Frequency of all SOs
Frequency of all spindles
Frequency of uncoupled spindles

3.3. APOE genotype modulates coupled sleep rhythms

In light of previous studies reporting that *APOE* genotype can modulate brain electrophysiological activity [33,34], we investigated whether *APOE* genotype has differential effects on the integrity of coupled sleep rhythms during AD progression. Compared to the *APOE* ε4 non-carriers, the frequency of SO-theta burst coupling and SO-spindle coupling decreased in the *APOE* ε4 carriers; SO-coupled theta burst and spindle power are lowered (ANCOVA; adjusted for age, gender, and education; all $P_{corrected}$ <0.05; Fig. 2a–d, Table S4 online). The preferred SO phases for coupled theta bursts and spindles differed between *APOE* ε4 carriers and non-carriers (Watson-Williams test: theta burst: $F_{1,93}$ = 5.27, $P_{corrected}$ = 0.029; spindle: $F_{1,93}$ = 28.81, $P_{corrected}$ < 0.001; Fig. 2e, f; Table S4 online). In a subgroup analysis, the effects of *APOE* genotype on coupled sleep rhythms were detected in the MCI population (Fig. 2a–f).

To further investigate the effect of *APOE* ε4 allele load on sleep rhythms, we performed a linear regression analysis, which indicated that an increased *APOE* ε4 load was associated with reduced SO-spindle coupling frequency (adjusted for age, gender, and education; β = –0.29, $P_{corrected}$ = 0.030; Table S5a online). Additionally, ANCOVA results showed that participants with the ε4/ε4 genotype exhibited a lower frequency of SO-spindle coupling than those with the ε3/ε4 genotype (adjusted for age, gender, and education; *MD* = –0.28, $P_{corrected}$ = 0.012; Table S5b online). These results suggest that *APOE*ε4 participates in the disruption of coupled sleep rhythms during AD progression.

3.4. Coupled sleep rhythm disruption is associated with amyloid and tau pathology

We built a linear regression model to assess relationships between coupled sleep rhythms and CSF AD biomarker levels (adjusted for age, gender, education, and *APOE* ε4 carrier status). The model indicated significant associations between coupled sleep rhythms and CSF Aβ42, p-tau181, and t-tau levels among the three populations (Fig. 2g, h; Table S6 online). Electrophysiological data on SO-theta burst coupling revealed significant associations with AD biomarkers. A decreased frequency of SO-theta burst coupling was associated with lower CSF Aβ42 levels (β = 0.25, $P_{corrected}$ = 0.026), and elevated levels of p-tau181 (β = –0.22, $P_{corrected}$ = 0.035) and t-tau (β = –0.38, $P_{corrected}$ = 0.001). Additionally, reduced SO-coupled theta burst power (β = 0.25, $P_{corrected}$ = 0.019) and greater misalignment of SO phase for coupled theta bursts (β = 0.29, $P_{corrected}$ = 0.012) were both associated with lower CSF Aβ42 levels.

Considering that AD pathology burden can be indexed by AD biomarker combinations (a higher burden indicates t-tau/Aβ42 exceeds the median, and otherwise a lower burden) [35,36], we explored whether changes in coupled sleep rhythms informatively reflect AD pathology burden. Individuals with high AD pathology burden showed decreases in the frequency of SO-theta burst coupling and SO-spindle coupling (ANCOVA; adjusted for age, gender, education, and *APOE* ε4 carrier status; SO-theta burst: *MD* = –3.36, $P_{corrected}$ = 0.001; SO-spindle: *MD* = –2.63, $P_{corrected}$ = 0.010; Fig. S7 online). The preferred SO phases for coupled theta bursts and spindles also differed between individuals with high versus low AD pathology burden (Watson-Williams tests: SO-theta burst: $F_{1,85}$ = 6.94, $P_{corrected}$ = 0.013; SO-spindle: $F_{1,85}$ = 12.86, $P_{corrected}$ < 0.001; Fig. S7 online). These findings suggest that coupled sleep rhythm disruption is associated with a higher AD pathology burden.

3.5. Coupled sleep rhythm disruption is associated with grey matter atrophy

We investigated the neuroanatomical basis potentially underlying the observed coupled sleep rhythm disruption in AD, focusing on the medial prefrontal cortex (mPFC), hippocampus, and thalamus—areas previously implicated in generating SOs [26], theta bursts [37], and spindles [38]. Partial correlation analysis indicated that decreases in SO-coupled theta burst power were associated with the grey matter volume of the hippocampus (adjusted for age, gender, education, *APOE* ε4 carrier status, and TIV; ρ = 0.46, $P_{corrected}$ = 0.018; Fig. 3a). A circular-linear correlation analysis indicated that the preferred SO phase for coupled spindles was associated with the grey matter volume of the mPFC (adjusted for age, gender, education, *APOE* ε4 carrier status, and TIV; ρ = 0.45, $P_{corrected}$ = 0.021; Fig. 3b). No associations with coupled sleep rhythms were found for the thalamus or control ROIs (e.g., orbitofrontal cortex, dorsolateral PFC, precuneus) (Fig. S8 online). These results support that atrophy of the hippocampus and the mPFC is involved in the disruption of SO-theta burst coupling and SO-spindle coupling during AD progression.

3.6. Coupled sleep rhythm disruption predicts cognitive decline in the AD dementia and MCI populations

Given that coupled sleep rhythms during NREM sleep support memory consolidation [5], we explored whether coupled sleep rhythm disruption impairs cognitive function during AD progression. A linear regression analysis indicated associations between coupled sleep rhythms and neuropsychological scores at baseline (CDR-sum of boxes [SB], the Mini-Mental State Examination, Montreal Cognitive Assessment, Auditory Verbal Learning Test, Backward Digit Span, and Trail Making Test-Part B), adjusting for age, gender, education, and *APOE* ε4 carrier status (Fig. 3c; Table S7 online). To further investigate these relationships, we performed CCA on variables that exhibited significant correlations. The first canonical component was significant (ρ = 0.58, P < 0.001), exceeding the null confidence interval after 10,000 permutations (P < 0.001) (Fig. S9 online). As shown in Fig. 3d, all sleep rhythm variables are located in the first quadrant, indicating their positive

Fig. 3. Associations of coupled sleep rhythm with grey matter atrophy and cognitive impairment. (a) Scatter plot showing that reduced SO-coupled theta burst power correlates with hippocampal grey matter atrophy, with the hippocampus ROI displayed on axial slices. (b) Scatter plot illustrating that preferred SO phase for coupled spindles correlates with mPFC grey matter atrophy. The mean mPFC grey matter volume relative to SO phase for spindles is shown with dark grey bars indicating mean volume. The mPFC ROI is displayed on axial slices. (c) Heatmap of associations between coupled sleep rhythm and neuropsychological scores in the AD dementia, MCI, and CN populations. (d) Canonical correlation analysis of coupled sleep rhythm and neuropsychological scores in the AD dementia, MCI, and CN populations. Statistical significance for panel (a) was determined using partial correlation analysis, for panel (b) using circular-linear correlation analysis, and for panel (c) using linear regression, with adjustments for age, sex, education, *APOE* ε4 carrier status, and multiple comparisons. Panel (d) employed canonical correlation analysis. AD: Alzheimer's disease; *APOE*: apolipoprotein E; AVLT: Auditory Verbal Learning Test; AVLT-C: AVLT-cued recall; AVLT-D: AVLT-delayed recall; AVLT-I: AVLT-immediate recall; AVLT-R: AVLT-recognition; BDS: Backward Digit Span; BNT: Boston Naming Test; CDR-SB: Clinical Dementia Rating sum of boxes; CDT: Clock Drawing Test; CN: cognitively normal; FDS: Forward Digit Span; GM: grey matter; MCI: mild cognitive impairment; mPFC: medial Prefrontal Cortex; MMSE: Mini-Mental State Examination; MoCA: Montreal Cognitive Assessment; NREM: non-rapid eye movement; ROI: region of interest; SO: slow oscillation; TMT: Trail Making Test.

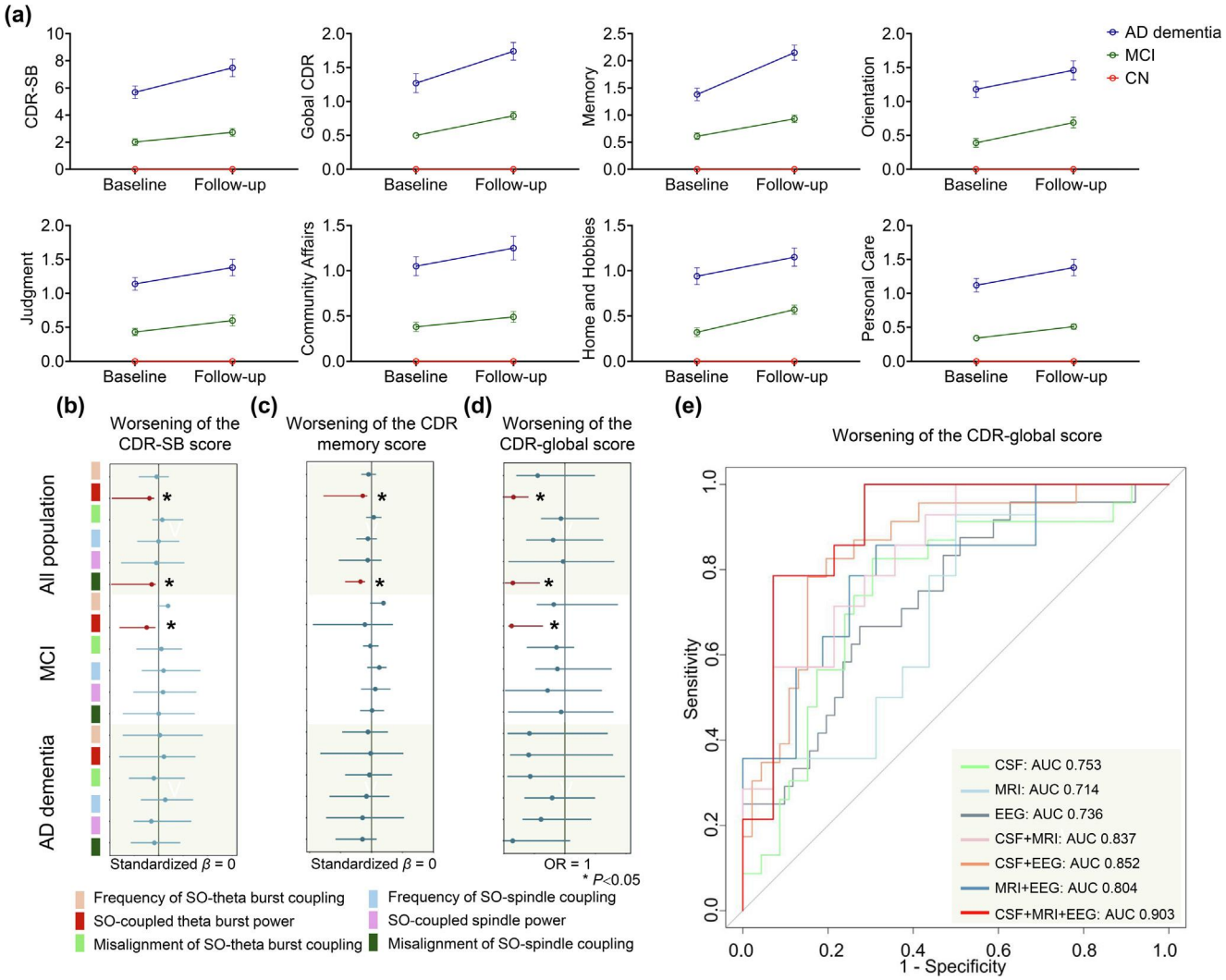

Fig. 4. Prognostic value of coupled sleep rhythm for cognitive decline in AD progression. (a) Cognitive trajectories over a two-year follow-up in the AD dementia, MCI, and CN populations, with data shown as medians and interquartile ranges. (b) Forest plot depicting the association of coupled sleep rhythm with changes in CDR-SB score (i.e., $CDR\text{-}SB_{follow\text{-}up}$ score minus $CDR\text{-}SB_{baseline}$ score [39]). (c): Same as panel (b), but for changes in CDR-memory score (i.e., $CDR\text{-}Memory_{follow\text{-}up}$ score minus $CDR\text{-}Memory_{baseline}$ score [40]). (d): Same as panel (c), but for changes in CDR-global score. Box and line indicate standardized β or adjusted OR with 95% CI. (e) ROC analysis for the prognostic value (measured by changes in CDR-global score) of various biomarker combinations for the three populations. Examined CSF biomarkers included the Aβ42/40 ratio, Aβ42, p-tau181, and t-tau levels. Examined MRI biomarkers included mPFC and hippocampal grey matter volumes. Examined EEG biomarkers included SO-coupled theta burst power and misalignment of SO-spindle coupling. Statistical significance for panels (b–c) was assessed using linear regression, while panel (d) was analyzed using logistic regression, with adjustments for age, sex, education, *APOE* ε4 carrier status, and multiple comparisons. AD: Alzheimer's disease; *APOE*: apolipoprotein E; AUC: area under curve; CDR: Clinical Dementia Rating; CDR-SB: Clinical Dementia Rating-sum of boxes; MCI: mild cognitive impairment; NREM: non-rapid eye movement; OR: odds ratio; SO: slow oscillation.

association with cognitive performance. This finding suggests that the first canonical variable effectively represents an overall cognitive function dimension, characterized by higher sleep rhythm values.

We then analyzed the relationship between coupled sleep rhythms and longitudinal changes in cognition over a two-year follow-up period (median follow-up: 27.4 months adjusted for age, gender, education, and *APOE* ε4 carrier status) (Fig. 4a and Table S8 online). A linear regression analysis indicated that a decrease in SO-coupled theta burst power was associated with worsening CDR-SB (β = −0.38, $P_{corrected}$ = 0.014) and CDR-memory scores (β = −0.29, $P_{corrected}$ = 0.031) (adjusted for age, gender, education, and *APOE*ε4 carrier status; Fig. 4b, c; Table S9 online). The misalignment of SO-spindle coupling was associated with worsening CDR-SB (β = −0.28, $P_{corrected}$ = 0.031) and CDR-memory scores (β = −0.36, $P_{corrected}$ = 0.021) (Fig. 4b, c; Table S9 online). A logistic regression analysis indicated that decreased SO-coupled theta burst power was associated with worsening of CDR-global scores (odds ratio [OR] = 0.16, $P_{corrected}$ = 0.013) and progression from MCI to AD dementia (OR = 0.13, $P_{corrected}$ = 0.027) (An OR < 1 indicates that lower EEG measure values are associated with higher odds of cognitive decline. Fig. 4d). Misalignment of SO-spindle coupling was associated with worsening of CDR-global scores (OR = 0.15, $P_{corrected}$ = 0.011) (Fig. 4d).

We used Receiver Operating Characteristic (ROC) analysis to evaluate the predictive value of coupled sleep rhythms for cognitive decline in AD. The identified coupled sleep rhythms (decreased SO-coupled theta burst power and misalignment of SO-spindle coupling) predict cognitive decline with an area under the curve (AUC) of 0.74 (95% CI: 0.62–0.86) (Fig. 4e; Fig. S10 online). To assess whether integrating EEG biomarkers can enhance the CSF and MRI biomarkers for AD progression, we calculated the AUC for CSF biomarkers: the AUC was 0.75 (95% CI: 0.63–0.88); for combined CSF and MRI biomarkers, the AUC

was 0.84 (95% CI: 0.69–0.98); for combined CSF, MRI, and EEG biomarkers, the AUC was 0.90 (95% CI: 0.81–0.99). These findings suggest that coupled sleep rhythm disruption during NREM sleep predicts accelerated cognitive decline. Further, integrating sleep EEG with CSF and MRI biomarkers enhances the predictive ability for AD progression. The EEG biomarkers also demonstrated discriminatory value between AD and CN controls (Fig. S11 online).

4. Discussion

We identified that coupled sleep rhythm disruption evolves during AD progression. Specifically, the frequency of SO-theta burst coupling and of SO-spindle coupling decreases from CN to MCI; SO-theta burst coupling and SO-spindle coupling further misaligns from MCI to AD dementia. The *APOE* ε4 allele and elevated amyloid and tau burden are associated with coupled sleep rhythm disruption. Hippocampal and medial prefrontal cortex atrophy are respectively linked to SO-theta burst coupling and SO-spindle coupling. Notably, coupled sleep rhythm disruption predicts accelerated cognitive decline over a two-year follow-up period. Finally, we found that integrating sleep EEG with CSF and MRI biomarkers enhances the predictive ability for AD progression.

Coupled sleep rhythm disruption during NREM sleep can negatively impact cognitive functions in healthy older adults [20,41,42]. Previous studies have shown that memory consolidation relies on the precise interaction of the coupled sleep rhythms during NREM sleep [1,43]. A longitudinal study on age-related changes in coupled sleep rhythms has shown an association with impaired memory performance over two years, specifically linked to the misalignment of the SO phase with spindles [41,44]. Studies of MCI patients have reported reduced theta burst power during the SO phase [21] and earlier spindle peak timing [42]. In AD, fewer spindles coupled with the SO upstate were linked to AD pathology and memory impairment [35,42]. Our study extends these findings, showing that disrupted SO-theta burst coupling and SO-spindle coupling are associated with accelerated cognitive decline during AD progression. However, the observational nature of our study limits causal conclusions. Randomized controlled trials targeting coupled sleep rhythms during NREM sleep, for example using functional electrical stimulation, will be necessary to determine whether restoring sleep rhythms can mitigate cognitive decline in AD.

Coupled sleep rhythms during NREM sleep, specifically the interaction between SOs, theta bursts, and spindles, are thought to arise from the interaction of thalamo-cortical and hippocampal-cortical communication [11,12,41,45]. Studies in healthy older adults indicate that mPFC atrophy predicts misalignment in SO-spindle coupling [41]. Positron emission tomography has shown that mPFC atrophy, associated with amyloid deposition, contributes to decreased temporal precision of SO-spindle coupling [20]. Our results extend this understanding to AD, showing that hippocampal and mPFC atrophy are linked to disruptions in SO-theta burst coupling and SO-spindle coupling. Studies in mice have implicated the hippocampus in generating theta bursts [46], and human studies suggest that reduced hippocampal volume decreases theta burst frequency and neuroplasticity [47]. Future studies utilizing magnetoencephalography or combined EEG-fMRI approaches would likely help clarify the directionality of related cortical-subcortical interactions, which cannot be fully captured by scalp EEG.

A range of biomarkers, including CSF proteins [48], neuroimaging [49], blood tests [50], and genetic risk profiles [51], can be used to improve the accuracy of AD diagnosis and to predict AD progression. In 2014, the International Working Group and the US National Institute on Aging-Alzheimer's Association proposed the incorporation of CSF and neuroimaging biomarkers into the diagnostic criteria for AD [52]. Studies have indicated that individuals with high levels of Aβ42 and t-tau have a significantly increased risk of progressing from MCI to AD [53,54]. Studies based on MRI have shown that decreases in hippocampal volume and cortical thickness can predict disease progression with more than 70% accuracy [55]. Our findings suggest that coupled sleep rhythms measured by EEG can further enhance the prognostic value of CSF and MRI biomarker systems for AD progression. Since EEG is non-invasive, portable, and capable of directly measuring neural activity, it holds promise as a tool for detecting and predicting biomarkers related to AD [34,56–59]. Further studies are needed to validate the use of EEG biomarkers for predicting AD progression.

This study has several limitations. First, as this study is observational, we cannot determine whether disrupted coupled sleep rhythms contribute to cognitive decline or simply reflect the progression of neurodegeneration in AD. Future randomized controlled trials using neuromodulation interventions targeting NREM sleep oscillations will be necessary to evaluate whether restoring oscillatory coupling can mitigate or slow cognitive decline. Second, our cognitive assessments were based solely on CDR performance, which may not be comprehensive. Additional scales or tasks are needed for a more thorough evaluation. Third, while the telephone interview for cognitive status is effective in detecting cognitive impairment [60–62], it lacks non-verbal assessments, such as the Clock Drawing Test, which provides valuable insights. Fourth, further studies should explore coupled sleep rhythm in larger cohorts and in populations with other types of dementia. Although our data included some measures of sleep continuity (e.g., sleep efficiency, wake after sleep onset), we acknowledge that a more detailed assessment of sleep fragmentation—such as arousal indices and the frequency of micro-awakenings—is necessary to determine whether changes in sleep oscillations are independently linked to cognitive decline or influenced by disrupted sleep. In future studies, these additional metrics should be included to provide a clearer understanding of this relationship. Fifth, sleep disturbances—such as sleep phase advance/delay—are commonly observed in AD and may contribute to variability in sleep oscillation metrics. Future studies with more extensive sleep profiling will be necessary to clarify their potential confounding effects on EEG-based analyses. Finally, caution is needed in generalizing our findings, as they are based on a single-center memory clinic. Replication in different populations and research centers will help mitigate selection bias.

In conclusion, our study characterized coupled sleep rhythms (i.e., SO-theta burst coupling and SO-spindle coupling) during AD progression. The presence of the *APOE* ε4 allele, along with elevated amyloid and tau burden, was associated with coupling alterations. Hippocampal and medial prefrontal cortex atrophy were associated with impairments in SO-theta burst coupling and SO-spindle coupling. Coupled sleep rhythm disruptions were associated with accelerated cognitive decline, improving the prognostic value of established AD biomarker systems. These findings deepen our understanding of the relationship between sleep and cognition in AD and suggest that coupled sleep rhythms could be a potential therapeutic target. Measures of coupled sleep rhythms during NREM sleep may have broader clinical utility in early detection, differential diagnosis, and in monitoring the effectiveness of interventions targeting sleep dysregulation in AD.

Conflict of interest

The authors declare that they have no conflict of interest.

Acknowledgments

This work was supported by the National Key Research and Development Program of China (2022YFC3602600 and 2023YFC3603200), the National Natural Science Foundation of China (82220108009, 32271093, and 82401664), Beijing Outstanding Young Scientist Program (JWZQ20240101023), STI2030-Major Projects (2021ZD0201801), and Beijing Hospitals Authority Youth Programme (QML20230802).

Author contributions

Yi Tang, Yunzhe Liu, Zhibin Wang, and Tao Wei participated in the study design. Tao Wei, Zhibin Wang, and Jianyang Zhou contributed to drafting the initial manuscript. Tao Wei, Jianyang Zhou, and Zhibin Wang conducted the statistical analyses and analyzed electrophysiological data. Tao Wei, Xiaoduo Liu, Yingxin Mi, Yiwei Zhao, Yi Xing, Bo Zhao, Shaojiong Zhou, and Yufei Liu contributed to the acquisition, processing and analysis of clinical data. Yi Tang, Yunzhe Liu, Zhibin Wang contributed to critical review of the manuscript for intellectual content. All authors reviewed and approved the final version of the manuscript.

Data availability

The datasets analyzed during the current study are available from the corresponding author on reasonable request.

Appendix A. Supplementary material

Supplementary data to this article can be found online at https://doi.org/10.1016/j.scib.2025.03.023.

References

[1] Diekelmann S, Born J. The memory function of sleep. Nat Rev Neurosci 2010;11:114–26.
[2] Rasch B, Born J. About sleep's role in memory. Physiol Rev 2013;93:681–766.
[3] Latchoumane CV, Ngo HV, Born J, et al. Thalamic spindles promote memory formation during sleep through triple phase-locking of cortical, thalamic, and hippocampal rhythms. Neuron 2017;95:424–35.
[4] Ngo HV, Fell J, Staresina B. Sleep spindles mediate hippocampal-neocortical coupling during long-duration ripples. Elife 2020;9:e57011.
[5] Staresina BP, Bergmann TO, Bonnefond M, et al. Hierarchical nesting of slow oscillations, spindles and ripples in the human hippocampus during sleep. Nat Neurosci 2015;18:1679–86.
[6] Shi L, Chen SJ, Ma MY, et al. Sleep disturbances increase the risk of dementia: a systematic review and meta-analysis. Sleep Med Rev 2018;40:4–16.
[7] Himali JJ, Baril AA, Cavuoto MG, et al. Association between slow-wave sleep loss and incident dementia. JAMA Neurol 2023;80:1326–33.
[8] Staresina BP. Coupled sleep rhythms for memory consolidation. Trends Cogn Sci 2024;28:339–51.
[9] Born J, Wilhelm I. System consolidation of memory during sleep. Psychol Res 2012;76:192–203.
[10] Schreiner T, Petzka M, Staudigl T, et al. Endogenous memory reactivation during sleep in humans is clocked by slow oscillation-spindle complexes. Nat Commun 2021;12:3112.
[11] Schreiner T, Doeller CF, Jensen O, et al. Theta phase-coordinated memory reactivation reoccurs in a slow-oscillatory rhythm during NREM sleep. Cell Rep 2018;25:296–301.
[12] Gonzalez CE, Mak-McCully RA, Rosen BQ, et al. Theta bursts precede, and spindles follow, cortical and thalamic downstates in human NREM sleep. J Neurosci 2018;38:9989–10001.
[13] Staresina BP, Niediek J, Borger V, et al. How coupled slow oscillations, spindles and ripples coordinate neuronal processing and communication during human sleep. Nat Neurosci 2023;26:1429–37.
[14] Jiang X, Gonzalez-Martinez J, Halgren E. Posterior hippocampal spindle ripples co-occur with neocortical theta bursts and downstates-upstates, and phase-lock with parietal spindles during NREM sleep in humans. J Neurosci 2019;39:8949–68.
[15] Steriade M. Grouping of brain rhythms in corticothalamic systems. Neuroscience 2006;137:1087–106.
[16] Rothschild G, Eban E, Frank LM. A cortical-hippocampal-cortical loop of information processing during memory consolidation. Nat Neurosci 2017;20:251–9.
[17] Sirota A, Csicsvari J, Buhl D, et al. Communication between neocortex and hippocampus during sleep in rodents. Proc Natl Acad Sci U S A 2003;100:2065–9.
[18] Maingret N, Girardeau G, Todorova R, et al. Hippocampo-cortical coupling mediates memory consolidation during sleep. Nat Neurosci 2016;19:959–64.
[19] Ashrafian H, Zadeh EH, Khan RH. Review on Alzheimer's disease: inhibition of amyloid beta and tau tangle formation. Int J Biol Macromol 2021;167:382–94.
[20] Chylinski D, Van Egroo M, Narbutas J, et al. Timely coupling of sleep spindles and slow waves linked to early amyloid-β burden and predicts memory decline. Elife 2022;11:e78191.
[21] Pulver RL, Kronberg E, Medenblik LM, et al. Mapping sleep's oscillatory events as a biomarker of Alzheimer's disease. Alzheimers Dement 2024;20:301–15.
[22] Wang C, Wang Z, Xie B, et al. Binaural processing deficit and cognitive impairment in Alzheimer's disease. Alzheimers Dement 2022;18:1085–99.
[23] Petersen RC, Negash S. Mild cognitive impairment: an overview. CNS Spectr 2008;13:45–53.
[24] McKhann GM, Knopman DS, Chertkow H, et al. The diagnosis of dementia due to Alzheimer's disease: recommendations from the National Institute on Aging-Alzheimer's Association workgroups on diagnostic guidelines for Alzheimer's disease. Alzheimers Dement 2011;7:263–9.
[25] Mak HK, Zhang Z, Yau KK, et al. Efficacy of voxel-based morphometry with DARTEL and standard registration as imaging biomarkers in Alzheimer's disease patients and cognitively normal older adults at 3.0 tesla MR imaging. J Alzheimers Dis 2011;23:655–64.
[26] Mander BA, Rao V, Lu B, et al. Prefrontal atrophy, disrupted NREM slow waves and impaired hippocampal-dependent memory in aging. Nat Neurosci 2013;16:357–64.
[27] Rajapakse JC, Giedd JN, Rapoport JL. Statistical approach to segmentation of single-channel cerebral MR images. IEEE Trans Med Imaging 1997;16:176–86.
[28] Tzourio-Mazoyer N, Landeau B, Papathanassiou D, et al. Automated anatomical labeling of activations in SPM using a macroscopic anatomical parcellation of the MNI MRI single-subject brain. Neuroimage 2002;15:273–89.
[29] Maldjian JA, Laurienti PJ, Kraft RA, et al. An automated method for neuroanatomic and cytoarchitectonic atlas-based interrogation of fMRI data sets. Neuroimage 2003;19:1233–9.
[30] Oostenveld R, Fries P, Maris E, et al. Fieldtrip: open source software for advanced analysis of MEG, EEG, and invasive electrophysiological data. Comput Intell Neurosci 2011;2011:156869.
[31] Delorme A, Makeig S. Eeglab: an open source toolbox for analysis of single-trial EEG dynamics including independent component analysis. J Neurosci Methods 2004;134:9–21.
[32] Gramfort A, Luessi M, Larson E, et al. MEG and EEG data analysis with MNE-Python. Front Neurosci 2013;7:267.
[33] de Frutos-Lucas J, Cuesta P, Ramírez-Toraño F, et al. Age and APOE genotype affect the relationship between objectively measured physical activity and power in the alpha band, a marker of brain disease. Alzheimers Res Ther 2020;12:113.
[34] Smailovic U, Johansson C, Koenig T, et al. Decreased global EEG synchronization in amyloid positive mild cognitive impairment and Alzheimer's disease patients-relationship to APOE ε4. Brain Sci 2021;11:1359.
[35] Hanert A, Schönfeld R, Weber FD, et al. Reduced overnight memory consolidation and associated alterations in sleep spindles and slow oscillations in early Alzheimer's disease. Neurobiol Dis 2024;190:106378.
[36] Jack Jr CR, Andrews JS, Beach TG, et al. Revised criteria for diagnosis and staging of Alzheimer's disease: Alzheimer's Association Workgroup. Alzheimers Dement 2024;20:5143–69.
[37] Bland BH. The physiology and pharmacology of hippocampal formation theta rhythms. Prog Neurobiol 1986;26:1–54.
[38] Steriade M, Domich L, Oakson G, et al. The deafferented reticular thalamic nucleus generates spindle rhythmicity. J Neurophysiol 1987;57:260–73.
[39] Bateman RJ, Smith J, Donohue MC, et al. Two phase 3 trials of gantenerumab in early Alzheimer's disease. N Engl J Med 2023;389:1862–76.
[40] Rentz DM, Rosenberg PB, Sperling RA, et al. Characterizing clinical progression in cognitively unimpaired older individuals with brain amyloid: results from the a4 study. J Prev Alzheimers Dis 2024;11:814–22.
[41] Helfrich RF, Mander BA, Jagust WJ, et al. Old brains come uncoupled in sleep: slow wave-spindle synchrony, brain atrophy, and forgetting. Neuron 2018;97:221–30.
[42] Ladenbauer J, Ladenbauer J, Külzow N, et al. Memory-relevant nap sleep physiology in healthy and pathological aging. Sleep 2021;44:zsab00.
[43] Walker MP, Stickgold R. Sleep, memory, and plasticity. Annu Rev Psychol 2006;57:139–66.
[44] Muehlroth BE, Sander MC, Fandakova Y, et al. Precise slow oscillation-spindle coupling promotes memory consolidation in younger and older adults. Sci Rep 2019;9:1940.
[45] Mikutta C, Feige B, Maier JG, et al. Phase-amplitude coupling of sleep slow oscillatory and spindle activity correlates with overnight memory consolidation. J Sleep Res 2019;28:e12835.

[46] Kilias A, Häussler U, Heining K, et al. Theta frequency decreases throughout the hippocampal formation in a focal epilepsy model. Hippocampus 2018;28:375–91.
[47] Vardalakis N, Aussel A, Rougier NP, et al. A dynamical computational model of theta generation in hippocampal circuits to study theta-gamma oscillations during neurostimulation. Elife 2024;12:RP87356.
[48] Forlenza OV, Radanovic M, Talib LL, et al. Cerebrospinal fluid biomarkers in Alzheimer's disease: diagnostic accuracy and prediction of dementia. Alzheimers Dement (Amst) 2015;1:455–63.
[49] Vipin A, Lee BTK, Kumar D, et al. The role of perfusion, grey matter volume and behavioural phenotypes in the data-driven classification of cognitive syndromes. Alzheimers Res Ther 2024;16:40.
[50] Palmqvist S, Tideman P, Cullen N, et al. Prediction of future Alzheimer's disease dementia using plasma phospho-tau combined with other accessible measures. Nat Med 2021;27:1034–42.
[51] Farhadieh ME, Mozafar M, Sanaaee S, et al. Polygenic hazard score predicts synaptic and axonal degeneration and cognitive decline in Alzheimer's disease continuum. Arch Gerontol Geriatr 2024;127:105576.
[52] Dubois B, Feldman HH, Jacova C, et al. Advancing research diagnostic criteria for Alzheimer's disease: the IWG-2 criteria. Lancet Neurol 2014;13:614–29.
[53] Hansson O, Zetterberg H, Buchhave P, et al. Association between CSF biomarkers and incipient Alzheimer's disease in patients with mild cognitive impairment: a follow-up study. Lancet Neurol 2006;5:228–34.
[54] Blom ES, Giedraitis V, Zetterberg H, et al. Rapid progression from mild cognitive impairment to Alzheimer's disease in subjects with elevated levels of tau in cerebrospinal fluid and the APOE epsilon4/epsilon4 genotype. Dement Geriatr Cogn Disord 2009;27:458–64.
[55] Aguilar C, Muehlboeck JS, Mecocci P, et al. Application of a MRI based index to longitudinal atrophy change in Alzheimer disease, mild cognitive impairment and healthy older individuals in the AddNeuroMed cohort. Front Aging Neurosci 2014;6:145.
[56] Meghdadi AH, Stevanović Karić M, McConnell M, et al. Resting state EEG biomarkers of cognitive decline associated with Alzheimer's disease and mild cognitive impairment. PLoS One 2021;16:e0244180.
[57] Vecchio F, Miraglia F, Alù F, et al. Classification of Alzheimer's disease with respect to physiological aging with innovative EEG biomarkers in a machine learning implementation. J Alzheimers Dis 2020;75:1253–61.
[58] Vecchio F, Miraglia F, Iberite F, et al. Sustainable method for Alzheimer dementia prediction in mild cognitive impairment: electroencephalographic connectivity and graph theory combined with apolipoprotein E. Ann Neurol 2018;84:302–14.
[59] Jiao B, Li R, Zhou H, et al. Neural biomarker diagnosis and prediction to mild cognitive impairment and Alzheimer's disease using EEG technology. Alzheimers Res Ther 2023;15:32.
[60] Chappelle SD, Gigliotti C, Léger GC, et al. Comparison of the telephone-montreal cognitive assessment (T-MoCA) and telephone interview for cognitive status (TICS) as screening tests for early Alzheimer's disease. Alzheimers Dement 2023;19:4599–608.
[61] Hlávka JP, Yu JC, Lakdawalla DN. Crosswalk between the mini-mental state examination and the telephone interview for cognitive status (TICS-27/30/40). Alzheimers Dement 2022;18:2036–41.
[62] Le JT, Agrón E, Keenan TDL, et al. Assessing bidirectional associations between cognitive impairment and late age-related macular degeneration in the age-related eye disease study 2. Alzheimers Dement 2022;18:1296–305.